

Nuclear Magnetic Resonance of F^{20} by Polarized Neutron Capture and β -Decay Anisotropy*

TUNG TSANG AND DONALD CONNOR

Argonne National Laboratory, Argonne, Illinois

(Received 17 June 1963)

The nuclear magnetic resonance of F^{20} ($T_{1/2}=11.4$ sec) has been observed by means of the polarized neutron capture, β -decay anisotropy technique. The nuclear g factor was found to be $+1.047 \pm 0.001$ nm/ \hbar (corrected for atomic diamagnetism). The principles of the experiment and the techniques used are discussed.

I. INTRODUCTION

WE report here some observations of the nuclear magnetic resonance (NMR) of the short-lived radio nuclide F^{20} by an unusual technique previously used only in a similar study of Li^8 by one of us.¹ The principles involved and the techniques used in the measurements are also discussed in some detail.

The basic NMR techniques due to Bloch and Purcell offer little for the study of nuclear magnetism in radioactive nuclides, despite their great value for stable nuclear species. The detection method is intrinsically macroscopic in nature, exploiting the electromagnetic field of the precessing nuclear magnetization. The limit of observability occurs at about 10^{20} spins of a given species. Such populations of radioactive nuclides are usually unattainable.

In selected cases, a million-fold greater sensitivity has been achieved by the use of electron-nuclear double resonance² methods [$(\mu_e/\mu_n)^2 \sim 10^6$]. The purely nuclear double-resonance methods due to Hahn and his associates³ may lead also to similar gains in some cases. Only rather long-lived radio nuclides may be studied even by these methods, however; for example, for half-life $T_{1/2}=25$ days, 10^{14} nuclei constitute 1 mCi of radioactivity.

Present knowledge of the magnetic properties of short-lived nuclides has been obtained almost entirely by other techniques, employing "triggered" detection methods.⁴ The most successful of these, the atomic-beam deflection measurement with target plates assayed by radiation counting, is applicable only if the daughter of the radio nuclide to be studied is also radioactive. The lower limit on half-lives seems to be about 1 h, imposed by the necessity for sample preparation.

A novel technique, peculiarly applicable to short-lived species, was used recently by one of us for a measurement of the nuclear g factor of Li^8 ($T_{1/2}=0.8$ sec). Connor¹ obtained Li^8 in a state of sizeable nuclear polarization ($\sim 10\%$) from the capture of polarized neutrons. He then carried out an NMR experiment,

using the asymmetry of the β decay as the indicator of nuclear polarization. The sensitivity of the method is illustrated by the fact that the Li^8 sample consisted of about 20 000 atoms (of course, continuously replenished).

We now have studied F^{20} ($T_{1/2}=11.4$ sec⁵) by the same technique. The sign and magnitude of the nuclear g factor have been determined and the resonance has been observed in a variety of compounds. We chose F^{20} for study primarily for reasons of convenience. Apart from Li^8 , it is the only nuclide for which we have yet found a substantial β -decay asymmetry at room temperature.⁶ However, the choice is also a reasonable one on the basis of physical interest. The simplest form of the shell model is quite useless in the vicinity of mass 20; various more sophisticated treatments have given contradictory results. By consideration of the hitherto neglected Coriolis term in the rotation Hamiltonian of the collective model, Kurath⁷ has now accounted closely for our results.

The following section is an analytical discussion of the experiment, summarizing the theory of the several phenomena involved in it. A third section presents some of the experimental details; these will be of interest primarily to others considering use of the technique. Our results are given in a fourth section, without interpretation in view of the following paper by Kurath.⁷

II. ANALYSIS OF THE EXPERIMENT

In outline, our method is this: polarized neutron irradiation of an F^{19} target produces F^{20} nuclei in a state of appreciable polarization, observable via the anisotropy of the F^{20} β decay (parity nonconservation). In crossed static and radio-frequency (rf) magnetic fields, the same combination conventional in NMR work, the nuclear polarization is perturbed in a frequency-dependent manner, so that the NMR of the F^{20} nuclei may be observed by a study of the β -decay asymmetry. In particular, the β -decay asymmetry will be partly destroyed when the frequency of the rf field is near the Larmor frequency. The geometry of the experiment is shown in Fig. 1. The level scheme of the $F^{19}-F^{20}-Ne^{20}$ system is shown in Fig. 2.

* Based on work performed under the auspices of the U. S. Atomic Energy Commission.

¹ D. Connor, Phys. Rev. Letters **3**, 429 (1959).

² G. Feher, C. S. Fuller, and E. A. Gere, Phys. Rev. **107**, 1462 (1957).

³ S. R. Hartmann and E. L. Hahn, Phys. Rev. **128**, 2042 (1962).

⁴ A. Abragam, *The Principles of Nuclear Magnetism* (Oxford University Press, New York, 1961), Chap. 1.

⁵ S. S. Glickstein and R. G. Winter, Phys. Rev. **129**, 1281 (1963).

⁶ A. H. Wapstra and D. Connor, Nucl. Phys. **22**, 336 (1961).

⁷ D. Kurath, Phys. Rev. **132**, 1146 (1963) (following paper).

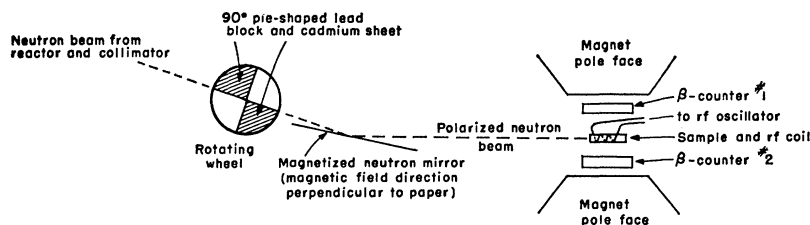


FIG. 1. Experimental layout.

A. Nuclear Polarization

Capture of slow neutrons ($L=0$) by nuclei of spin I gives the compound states, $I' = I - \frac{1}{2}$ and $I' = I + \frac{1}{2}$. The formation probability (cross section) of one compound state may be much greater than that of the other; presently the relative cross sections are usually unpredictable. For either process with unpolarized neutrons the several magnetic substates, $M' = I', M' = I' - 1, \dots, M' = -I'$, are formed with equal probability. Then $W(M_k')$, the relative probability of the substate M_k' , is independent of k , and the polarization $P \equiv \sum M_k' W(M_k') / I' \sum W(M_k')$ is zero. With polarized neutrons, however, the $W(M_k')$ are not equal and $P \neq 0$. In fact, we have

$$I' = I - \frac{1}{2}; \quad W(M_k') = (1 + I' - M_k') / 2(1 + I'),$$

$$\begin{cases} P = 0 & (I' = 0) \\ P = -\frac{1}{3} & (I' \neq 0) \end{cases} \quad (1)$$

$$I' = I + \frac{1}{2}; \quad W(M_k') = (I' + M_k') / 2I',$$

$$P = (1 + I') / 3I'.$$

The binding energy of the captured neutron appears as excitation of the compound nucleus, typically ~ 7 MeV, and the transition to the ground state (g.s.) occurs with the emission of one or more capture gamma rays. The angular momentum transfer associated with the gamma emission results in a g.s. polarization which

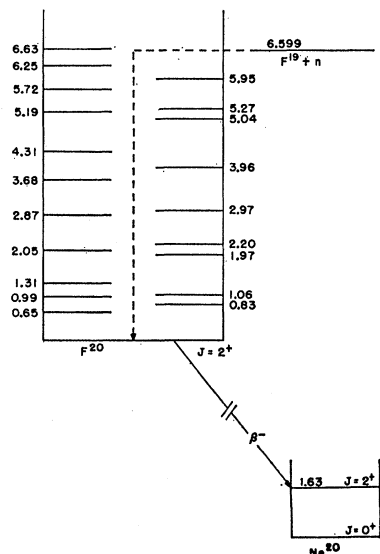


FIG. 2. $F^{19}-F^{20}-Ne^{20}$ level scheme. [According to F. Ajzenberg-Selove and T. Lauritsen, Ann. Rev. Nucl. Sci. 10, 409 (1960).]

differs from that given by (1). The decay-scheme data needed for its calculation are rarely available and we will not quote the results.⁸ In most cases, the g.s. polarization arising from capture into either compound state exceeds 0.1 in magnitude, so that the experimenter has reason for optimism. The polarization associated with one value of I' is opposite in sign to that associated with the other so that cancellation may diminish the net polarization in the ground state; it is probably rare for the effect to be appreciable, however.

B. β -Decay Anisotropy

We consider only allowed transitions for which the angular distribution is given⁹ by

$$W(\theta) = 1 + (v/c)PA \cos \theta, \quad (2)$$

where the coefficient A is a function of ΔI for the β transition and takes values listed in Table I.

If β particles emitted according to the distribution (2) are detected by a pair of similar counters, each subtending at the source a cone of half-angle θ_1 about the polarization axis, the relative difference in counting rates will be

$$(N_1 - N_2) / (N_1 + N_2) = (\alpha/2) \sin^2 \theta_1 / (1 - \cos \theta_1), \quad (3)$$

where $\alpha \equiv (v/c)PA$.

In our experiment, source and counters are in a strong magnetic field and $\theta_1 \approx \frac{1}{2}\pi$, so that

$$(N_1 - N_2) / (N_1 + N_2) \approx \frac{1}{2}\alpha.$$

When magnetic relaxation is negligible, the value of α should lie in the range 0.01 to 0.5.

C. Nuclear Magnetic Resonance

The nuclear polarization \mathbf{P} gives rise to the magnetization $\mathbf{M} = \mu\rho\mathbf{P}$, where μ is the nuclear magnetic dipole moment and ρ is the density of polarized nuclei. One expects that the phenomenon of nuclear magnetic resonance will occur if the usual combination of magnetic fields is provided; namely, a static field \mathbf{H}_0 along the initial polarization \mathbf{P}_0 and an rf field \mathbf{H}_1 at right angles to it. Under these conditions, \mathbf{M} and, therefore, \mathbf{P} , will depend on the rf field strength H_1 and its frequency ω . The relative counting rates are sensitive only to P_z , we thus limit our attention to M_z (the z axis is taken along \mathbf{P}_0).

⁸ F. D. Shapiro, Usp. Fiz. Nauk. 65, 133 (1958).

⁹ E. J. Konopinski, Ann. Rev. Nucl. Sci. 9, 99 (1959).

TABLE I. Asymmetry coefficient A for allowed β emission with angular-momentum change ΔI . I'' is the spin of the parent nucleus.

I	A
1	$I''/(1+I'')$
-1	-1
0	$-1/(1+I'')$ (pure G-T)
0	0 (pure Fermi)

We may write a rate equation¹⁰ for M_z ,

$$\dot{M}_z = \mu P_0 K - M_z[\tau^{-1} + T_1^{-1} + \pi\gamma^2 H_1^2 f(\omega)], \quad (4)$$

where the first term on the right gives the contribution due to polarized neutron capture at the rate K per cm³-sec, and the second the loss due to β decay with mean life τ . The third term accounts for relaxation of M_z with characteristic time T_1 , the "spin-lattice" relaxation time of NMR theory. The effect of the rf field H_1 is given by the fourth term, γ being the nuclear gyromagnetic ratio and $f(\omega)$ a line-shape function which measures the strength of the absorption at frequency ω . In a steady-state experiment, $\dot{M}_z = 0$ so that

$$M_z = \mu P_0 K / [\tau^{-1} + T_1^{-1} + \pi\gamma^2 H_1^2 f(\omega)]. \quad (5)$$

It is noteworthy that the β lifetime τ and the relaxation time T_1 appear on an equal footing in (4) and (5). Since the density of polarized nuclei is $\rho = K\tau$, we get:

$$P_z = M_z / \mu K \tau = P_0 / [1 + \tau T_1^{-1} + \pi\tau\gamma^2 H_1^2 f(\omega)]. \quad (6)$$

Experimentally, we determine the apparent asymmetry parameter α' , given by

$$\alpha' / \alpha_0 = P_z / P_0 = [1 + \tau T_1^{-1} + \pi\tau\gamma^2 H_1^2 f(\omega)]^{-1}. \quad (7)$$

The calculation of $f(\omega)$ is an unsolved problem although its moments have been obtained.^{11,12} Empirically, in solids it may be described qualitatively as intermediate between the Gaussian and Lorentzian shapes. For F²⁰ in CaF₂¹⁹, a calculation using the F²⁰ gyromagnetic ratio given in Sec. IV gives the ratio of the fourth moment to the square of second moment as approximately 13, indicating a nearly Lorentzian shape.¹³ (For Gaussian shapes the ratio is 3.) The dependence of α' on ω and H_1 to be expected for a Lorentzian $f(\omega)$ is shown in Fig. 3. Here the line shape is taken to be

$$f_L(\omega) = \delta\pi^{-1} [\delta^2 + (\omega - \omega_0)^2]^{-1}, \quad (8)$$

¹⁰ See, for example, a review by A. Abragam, in *The Principles of Nuclear Magnetism* (Oxford University Press, New York, 1961), Chap. 12.

¹¹ J. H. Van Vleck, *Phys. Rev.* **74**, 1168 (1948).

¹² D. E. O'Reilly and T. Tsang, *Phys. Rev.* **128**, 2639 (1962).

¹³ This difference in F²⁰ line shape as compared to F¹⁹ is due to the much smaller gyromagnetic ratio of F²⁰. See, for example, the discussion by A. Abragam, in *The Principles of Nuclear Magnetism* (Oxford University Press, New York, 1961), p. 122.

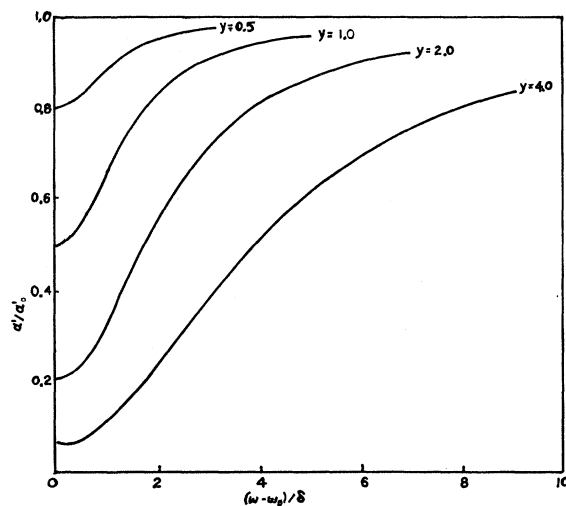


Fig. 3. Resonance observations to be expected if absorption is Lorentzian. [This is a plot of Eq. (9), with $y = \gamma H_1 \tau^{1/2} \delta^{-1/2} \times (1 + \tau T_1^{-1})^{-1/2}$.]

so that

$$\alpha' = \alpha_0' \left[1 + \frac{\tau\delta}{1 + \tau T_1^{-1}} \frac{\gamma^2 H_1^2}{\delta^2 + (\omega - \omega_0)^2} \right]^{-1}, \quad (9)$$

$$\alpha_0' \equiv \alpha_0 (1 + \tau T_1^{-1})^{-1}.$$

In (9), α' and α_0' are the observed asymmetry in the presence and in the absence of H_1 , respectively.

III. EXPERIMENTAL PROCEDURE

A. Neutron Polarization

The polarized neutron beam is obtained by reflection of reactor thermal neutrons from a magnetized cobalt alloy mirror. Our mirror is similar in design to that described by Burgy *et al.*¹⁴ Its use has offered little difficulty; the initial alignment is tedious but straightforward.

Measurement of the neutron polarization has been more troublesome. Our results indicate a value of about 0.8. We have used the Hughes technique of comparing the reflected intensities from a second mirror with and without depolarization of the beam in the region between the two mirrors.¹⁴ The depolarization is easily obtained by passage through a thin unmagnetized iron foil (usually 8-mil shim steel). The results obtained are quite sensitive to small shifts in alignment of the mirrors, to beam collimation at the second mirror, and to the location of the iron foil. Other approaches seem preferable and we plan further work. The problem takes rather low priority, however, since our NMR results do not depend on the value of the neutron polarization (as long as the effect is observable!).

A mirror reflects a reasonable fraction of the thermal

¹⁴ M. T. Burgy, V. E. Krohn, T. B. Novey, G. R. Ringo, and V. L. Telegdi, *Phys. Rev.* **120**, 1829 (1960).

neutron spectrum only at very low angles of incidence, 8 min of arc representing a fair compromise between mirror length and reflectivity. At this angle our 125-cm mirror gives only 3-mm-beam width. No comparable restriction is imposed on the other dimension of beam cross section and the total intensity increases directly with it, so that the "natural" shape of the beam cross section is an elongated rectangle, 3 mm by 5 cm in our equipment. The convenient direction of mirror magnetization polarizes the neutrons parallel to the long dimension of the beam section.

Polarization parallel to the small beam dimension is desirable at the sample in order to minimize the effect of scattering in the sample upon the observed β -particle asymmetry. We achieve this by a 90° rotation of the beam polarization along the flight path between mirror and target, using a simple configuration of permanent magnets to provide a "guide" field of about 400 Oe which rotates through 90° in 15 cm of beam path. Since the Larmor precession distance in 400 Oe is only 2 mm, no appreciable depolarization results. Elsewhere along the beam path, guide fields of about 100 Oe are provided.

The reflected beam intensity is about 10^7 polarized neutrons/sec.

B. Neutron Beam Chopping

The neutron capture which gives the polarized radioactive sample is accompanied by the emission of energetic capture gamma rays. In order to avoid a serious contribution to the beta counter background, irradiation and counting periods are separated by alternately gating of the neutron beam and the beta counters. The neutron gate is a rotating shutter between the reactor and the mirror. A thin cadmium sheet (0.02 in.) suffices to absorb the thermal neutron beam but we use 10 in. of lead as well, in order to eliminate the gamma-ray background due to the reactor.

Elementary analysis shows that equal periods for irradiation and counting are optimum and that the cycle duration should be short compared to τ . For F^{20} ($\tau=16$ sec) the beam shutter is operated at 60 rpm, giving 2 neutron bursts/sec.

C. Sample Environment

The magnetic field H_0 at the sample is required to be moderately intense and homogeneous. These conditions are most readily satisfied by the use of a large electromagnet of the type used for conventional NMR work. A rather large gap is required because of the scintillation counters. We use a 12-in. magnet¹⁵ with the poletips removed, giving a gap of $5\frac{1}{2}$ in. A proton resonance gaussmeter is used for measurement of H_0 .

The target material is supported by a thin ($\frac{1}{2}$ -mil) Teflon envelope, stretched inside a molded plastic frame. The rf coil is wound about the frame. The assembly is shown in Fig. 4. The rf coil design gives fair homogeneity

¹⁵ Model V-4012A, Varian Associates, Palo Alto, California.

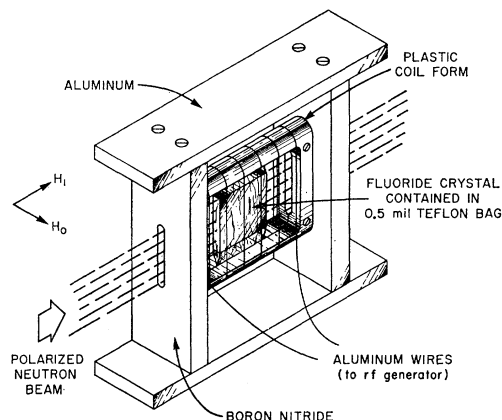


FIG. 4. Target/coil form assembly. Neutron and nuclear polarization are parallel to H_0 .

of H_1 (10%) while conserving space in the magnetic gap.

The counters are conventional plastic scintillators, connected by long light pipes to photomultipliers mounted well out of the magnet gap. All the experiments were carried out at room temperature.

D. Choice of Target Materials

Two considerations are important, apart from the obvious requirement that the desired target nucleus be present. Neutron capture by the other nuclei present in the sample may lead to interfering beta activities, a sort of built-in background. Also, spin-lattice relaxation seriously attenuates the observable β -decay asymmetry unless $T_1 \gtrsim \tau$. Relaxation due to magnetic interactions depends on the presence of paramagnetic impurities; pure materials are therefore desirable. Relaxation due to the electric quadrupole interaction is least in ionically bound compounds.

CaF_2 is a good choice for F^{19} targets, since Ca has a small activation cross section, very pure single crystals are available, and the binding is ionic. The use of single crystals also offers the opportunity of studying the orientation dependence of the line shape. Scattering of neutrons by the target is also minimized by the use of single crystals. In most of our work Harshaw CaF_2

TABLE II. β -decay asymmetries for different compounds at $H_0=5$ kG.

Compound	% Asymmetry	% Asymmetry for CaF_2 under similar conditions
NaF crystal	4.2 ± 0.5	4.2 ± 0.3
KF crystal	4.5 ± 0.3	4.2 ± 0.3
MgF_2 crystal	3.7 ± 0.3	3.68 ± 0.17
BaF_2 crystal	1.2 ± 0.3	4.2 ± 0.3
PbF_2 powder	0.5 ± 0.3	4.2 ± 0.3
Teflon	-0.1 ± 0.1	2.8 ± 0.1
FC-75 Fluorocarbon liquid	0.04 ± 0.04	2.8 ± 0.1

crystals were used although we also made brief studies with a variety of other compounds.

E. Measurement Procedure

As one sees from Eq. (7), the basic quantity to be measured is the relative difference in rates of the two beta counters with H_0 , H_1 , and ω appearing as controlled parameters. However, in order to correct for the slow relative drift of the counters, as well as other possible departures from precise symmetry in the apparatus, we always use the comparison between successive counts with the polarized neutron beam and with the beam depolarized by passage through an unmagnetized iron foil. The rather small asymmetry ($\alpha_0=0.04$) and low intensity due to the small capture cross section of F¹⁹ required counting periods of the order of 16 h per data point, and we have used an automatized arrangement in which the neutron polarization was switched every 3 min.

The search for a totally unknown resonance resembles the celebrated needle/haystack problem. The relative linewidth is of the order 10^{-3} while the position can be estimated no better than within a factor of two. Thus, an entirely naive approach might require thousands of hours. Instead, we swept the "static" magnetic field over a range of 200 G at 1 cps, using a fairly large H_1 (~ 1 Oe). With this scheme, if the resonance lies within the sweep range, essentially complete depolarization occurs once per second and the average asymmetry is reduced by the factor $\frac{1}{2}\tau^{-1}\sim 0.05$. With the resonance located to within the sweep range of 200 Oe, successive reductions of the range improve the precision of location until point by point study of the resonance curve becomes feasible. Our procedure for measurement of the sign of the magnetic moment has been described elsewhere.¹⁶

With typical targets, CaF₂ crystals about $0.2\times 2.5\times 2.5$ cm³, counting rates were of the order of 100/sec for each counter. The actual number of F²⁰ atoms in the target was thus of the order of 10 000, illustrating the remarkable sensitivity of the method.

IV. RESULTS

A. β -Decay Asymmetry

The observed asymmetry α_0' for F²⁰ β decay in CaF₂ crystals ($H_0=5014$ Oe parallel to 111 axis) vary between 2.8 ± 0.1 and $5.1\pm 0.4\%$ depending on the β -counter pulse-height discriminator setting. The higher asymmetry figure is obtained by selecting only the largest pulses, corresponding to the most energetic β particles. Wapstra and Connor⁶ observed a value of $2.2\pm 0.3\%$ with similar but cruder experimental conditions.

The asymmetry was measured for a variety of other fluorine compounds. The results are given in Table II,

¹⁶ D. Connor and T. Tsang, Phys. Rev. **126**, 1506 (1962).

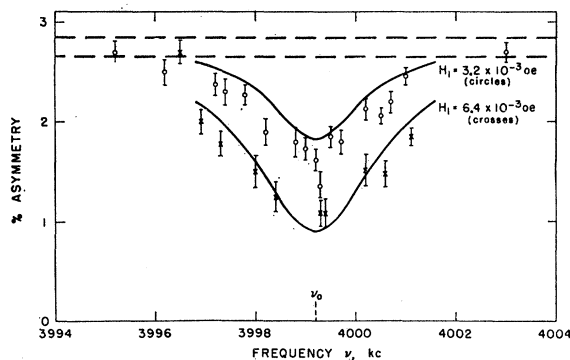


FIG. 5. Experimental NMR asymmetry data, CaF₂ ($H_0\parallel 111$ axis, 5013.8 ± 0.3 Oe). Experimental data and also resonance line shapes calculated from (9) using $\delta=0.9$ kc/sec and $\alpha_0=4.1\%$ are shown. Dashed lines indicate asymmetry (with experimental uncertainties) in the absence of rf field.

along with the CaF₂ value corresponding to the conditions of each measurement. The other ionic crystals (NaF, KF, MgF₂) give results quite comparable to CaF₂, while the more covalently bound BaF₂ and PbF₂ show markedly lower asymmetries. The purely covalent fluorocarbons show no significant asymmetry. These results are all explicable on the assumption that F²⁰ has a fairly large quadrupole moment, the observed asymmetry being controlled by the strength of quadrupolar spin-lattice relaxation.

B. Nuclear g Factor

Typical NMR data for CaF₂ crystals are shown in Figs. 5 and 6 for two values and orientation of H_0 relative to the crystal axes. The solid curves in the figures were calculated from (9), that is, assuming the line shape to be Lorentzian. The parameter values used for the calculation were $\delta=0.9$ kc/sec (Fig. 5), $\delta=1.5$ kc/sec (Fig. 6), and $\alpha_0=4.1\%$. These values for the width parameter are consistent with our estimate of

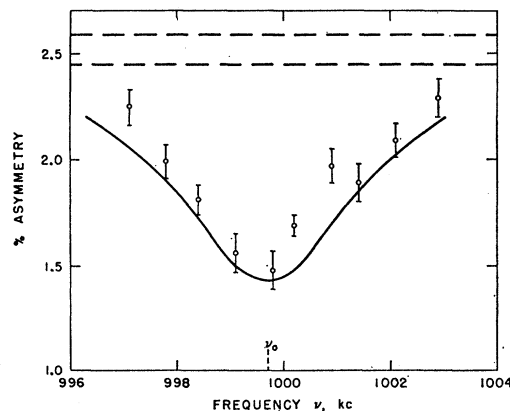


FIG. 6. Experimental NMR asymmetry data, CaF₂ ($H_0\parallel 110$ -axis, 1253.4 ± 0.5 Oe). $H_1=5.3\times 10^{-3}$ Oe. Experimental data and also resonance line shapes calculated from (9) using $\delta=1.5$ kc/sec and $\alpha_0=4.1\%$ are shown. Dashed lines indicate asymmetry (with experimental uncertainties) in the absence of rf field.

the broadening to be expected from the dipolar interaction with the F^{19} moments. We have also observed the resonance in a NaF crystal at the same Larmor frequency.

In a separate experiment, we determined the sign of the F^{20} moment to be positive by comparing the depolarization produced by left and right hand circular polarization of H_1 .¹⁶ With $\omega/2\pi=4$ Mc/sec, the resonance frequency in 5015 Oe, we found $\alpha'=2.2\%$ ($\omega\parallel\mathbf{H}_0$) and $\alpha'=1.2\%$ ($-\omega\parallel\mathbf{H}_0$). α_0' was 2.8%. The slight depolarization for the case $\omega\parallel\mathbf{H}_0$ is due to imperfect circular polarization of the rf field.

From the data represented in Figs. 5 and 6 we find the Larmor frequency to be 3999.2 ± 0.4 kc/sec in 5013.8 ± 0.3 Oe and 999.7 ± 0.4 kc/sec in 1253.4 ± 0.5 Oe. Without diamagnetic correction, the gyromagnetic ratio is, thus, $\gamma=+797.6\pm 0.2$ cps/Oe and the nuclear g factor, $g=\mu/\hbar I$, is $g=+1.0463\pm 0.0002$ nm/ \hbar . Making the small correction for atomic diamagnetism, we obtain $g=+1.047\pm 0.001$ nm/ \hbar . Since $I=2$,¹⁷ the magnetic moment is $\mu=+2.0926\pm 0.0004$ nm (uncorrected) or $\mu=+2.094\pm 0.002$ nm (corrected).

¹⁷ E. Freiberg and V. Soerbel, Z. Physik **162**, 114 (1961).

Ground State of $F^{20}\dagger$

DIETER KURATH*

University of Washington, Seattle, Washington

(Received 17 June 1963)

It is shown that in order to describe some properties of the F^{20} ground state, the $K=1$ and $K=2$ states of the Nilsson model must be strongly mixed. The primary ingredient in the description is, therefore, the rotational Coriolis term rather than the interaction between the odd neutron and odd proton.

INTRODUCTION

THE nucleus F^{20} lies in a region where a considerable amount of interpretation of nuclear properties has been carried out. This has been done either by means of a spherical shell model with residual two-body interactions or by means of the model of independent nucleons in a potential well of quadrupole deformation. The relationship between these interpretations has been demonstrated by means of the generating procedure,¹ and explicit calculations² showing their similarity have been done for nuclei of mass 18 and 19. The model with particles in a nonspherical potential well³ is much easier to apply and generally gives the important features of the lowest states, so it is employed in the following treatment.

The model for odd-odd nuclei is that of a deformed core to which both the odd proton and the odd neutron are strongly coupled. There are then two states for the neutron-proton system, one with parallel projections of angular momentum on the nuclear-symmetry axis, the other with antiparallel projections. Rotational bands exist for each of these internal states and the energy separation of the bands is determined both by the rotational Hamiltonian and by the neutron-proton interaction.

Gallagher and Moszkowski⁴ studied the heavy odd-odd nuclei, and concluded that the lowest state appeared in the majority of cases to be consistent with the predictions of a neutron-proton force which preferred to align the intrinsic spins of the neutron and proton. While the rotational-energy differences are of secondary importance for the heavy nuclei, for light nuclei like F^{20} , the rotational energy ($\hbar^2/2\mathcal{J}$) has an order of magnitude of several hundred keV compared to tens of keV in the heavy nuclei. Therefore, the rotational terms are of greater importance, and in cases like F^{20} where the resultant states of the neutron-proton system can be mixed by the rotational Hamiltonian this mixing will be the dominant feature.

II. PROPERTIES OF THE F^{20} GROUND STATE

From the preceding paper⁵ we know that the gyromagnetic ratio of F^{20} is $g=+1.046$. The angular momentum is $I=2^+$ (or 3^+) and the state decays⁶ by an allowed beta transition to the first excited state ($I=2^+$) of Ne^{20} with a value of $\log ft=4.99$.

The Nilsson³ picture for F^{20} is that of a core with prolate deformation, the odd-proton lying in level No. 6 with $k=\frac{1}{2}$ and the odd neutron in level No. 7 with $k=\frac{3}{2}$. The resultant neutron-proton states have projections of angular momentum $K=1$ and $K=2$ on the

[†] Supported in part by the U. S. Atomic Energy Commission.

* Permanent address: Argonne National Laboratory, Argonne, Illinois.

¹ J. P. Elliott, Proc. Roy. Soc. (London) **A245**, 128 and 562 (1958).

² M. G. Redlich, Phys. Rev. **110**, 468 (1958).

³ S. G. Nilsson, Kgl. Danske Videnskab. Selskab, Mat. Fys. Medd. **29**, No. 16 (1955).

⁴ C. J. Gallagher, Jr. and S. A. Moszkowski, Phys. Rev. **111**, 1282 (1958).

⁵ T. Tsang and D. Connor, Phys. Rev. **132**, 1141 (1963) (preceding paper).

⁶ D. Alburger, Phys. Rev. **88**, 1257 (1952).